Human-computer Interaction Perspectives on Condition Monitoring and Fault Diagnosis of Gearbox in Doubly-Fed Wind Turbines: An Exploration with Artificial Intelligence Technology

Ting Wang[1], Zhi-Hui Liu[2] and Jing Fan[3*]

[1,2]Engineering college, Applied Technology College of Soochow University, Suzhou, Jiangsu, 215000, China

[1]wting0714@163.com,[2]ZhiHuiLiu202308@outlook.com

[3]Electronic Information Engineering, Suzhou Vocational University, Suzhou, Jiangsu, 215000, China

Corresponding Author: Jing Fan, JingFan202308@outlook.com

Abstract. Monitoring the generator current is a convenient and quick fault detection method to find motor faults in a timely and convenient manner and maintain the regular operation of the generator set. This paper combines artificial intelligence technology to detect the gearbox status of doubly-fed wind turbines and uses technology to see whether there is a fault. Moreover, this paper studies the primary content of vibration monitoring, the calculation and physical meaning of time domain parameters for condition monitoring, and the method of practical value preprocessing. Aiming at the problem of impulsive impulses with suspected faults in the valuable value map caused by the sudden noise generated by the external environmental interference of the wind turbine gearbox, the standard distribution principle method is used to filter out the impulsive noise and construct an intelligent system. The simulation research shows that the innovative system proposed in this paper can effectively extract the fault features of the doubly-fed wind turbine.

Keywords: artificial intelligence; doubly-fed wind turbine; gearbox status; monitoring; fault diagnosis; Human-computer Interaction.
DOI: https://doi.org/10.14733/cadaps.2024.S20.252-267

1 INTRODUCTION

With the continuous growth of the development of wind power technology, the installed capacity of wind power is also increasing. Moreover, many problems in wind power generation have gradually emerged. The research and application of domestic wind turbine condition monitoring and fault diagnosis technology is still in its infancy, and it is far from keeping up with the rapid development of wind power installed capacity. There are more and more large-scale wind turbines, and it is not

easy to find the cause after failure, which has caused considerable losses to the operation of the entire unit. Wind farms are generally remote and scattered, and the units are on top of high towers.

Moreover, conventional vibrations such as acceleration and displacement, sensor installation and maintenance, and signal collection and transmission could be more convenient, making promoting wind turbine monitoring and diagnosis onerous. Suppose wind turbine detection and diagnosis can be done by detecting generator currents. In that case, many defects in vibration detection can be solved, physical damage to wind turbines can be reduced, and the ground can be seen without opening the wind turbine cabin.

To better use wind energy, wind turbines are usually installed at wind outlets where wind resources are concentrated, such as the Gobi Desert, islands, and other areas with harsher natural conditions in the northwest. These areas usually have a significant difference in temperature between day and night, and the direction and intensity of the wind also change from time to time, so the wind turbine is constantly impacted by strong winds with variable directions and loads during operation [5]. The harsh environment is the main external factor in the failure of wind turbines. In Chinese wind farms, the commonly used types of wind turbines are mainly divided into two categories. Gearboxes drive the first type. The production technology of this type of wind turbine is relatively mature and is currently the most widely used model in domestic wind farms. The second category is the model without a gearbox drive. Because it lacks the traditional part of the gearbox, the unit's volume is reduced, and the failure rate and maintenance cost are also significantly reduced [19].To connect the direct-drive wind turbine to the power grid, a full-power power electronic converter needs to be installed, and the price of the converter is relatively high. Compared with the first type of model, the running cost of the wind turbine is higher [6].

Currently, the mainstream models of domestic wind farms are still megawatt-level, double-fed asynchronous generators driven by gearboxes. This type of machine has a high utilization factor of wind resources, and the impact current on the enormous power grid is small when connected to the grid. Still, its failure rate is also high, increasing the wind farm's power generation cost. How to reduce the failure rate of units and reduce the cost of power generation has become the most concerning and urgent problem in this field. Wind turbine faults can be divided into electrical, communication, and mechanical. Among them, mechanical faults mainly include impeller faults and transmission system faults. The gearbox is the most essential part of the transmission system. It is a heavy-duty, speed-increasing transmission device composed of gears, bearings, and shafting. The data shows that the component with the highest failure rate in wind turbines is the gearbox, and the failure rate is increasing year by year.

This paper combines artificial intelligence technology to detect the state of the gearbox of the doubly-fed wind turbine. It sees whether there is a fault to improve the operation effect of the gearbox of the doubly-fed wind turbine.

2 RELATED WORK

With the development of motor and wind power generation technology, some scholars and researchers have conducted extensive research and discussion on motor faults and wind power generation fault detection [14]. Although some scholars and researchers have proposed many wind turbine fault diagnosis and detection methods, there are few practical applications in wind power [3]. The development of foreign countries is worthy of domestic study and reference. Some articles analyzed the basic principles of motor equipment fault diagnosis and proposed diagnostic methods based on signal transformation, expert systems, fuzzy theory, artificial neural networks, and integrated intelligent systems [6]. Due to the uncertainty of motor faults, they also proposed the multi-sensor fusion method and the current detection method [1]. Detecting the current of the rotor and stator of the motor and performing spectrum analysis on the collected current signal can protect

the motor's peak current detection and protection circuit. It can also perform online monitoring for rotor eccentricity, broken bars, cracked rings, interphase short circuits, open circuits, and other faults [9]. The current detection method can more accurately understand the working condition of the motor. When the motor fails, the current will change very sensitively, so the current detection of the motor fault is a very effective fault detection method. The motor and the generator have similarities in principle, and their fault diagnosis also has similarities. Regarding the vibration of large wind turbines, including gearbox vibration, scientific researchers have done scientific analysis to clarify the location and vibration mechanism of the units prone to failure and provide a basis for fault diagnosis [15]. The fault diagnosis of wind turbines is mostly based on vibration methods. There are few research reports on sensorless diagnosis methods, most of which are preliminary studies. Literature [13] established a wind turbine fault diagnosis and monitoring system based on generator electrical signals, assisted in monitoring vibration and temperature signals, and conducted preliminary experimental research. Literature [7] studies and analyzes the current and voltage signal fault characteristics of doubly-fed, cage-type, and direct-drive induction generator sets when mechanical and electrical faults occur, modeling and simulating the fault state of the main components of the generator and verifying the generator set. The accuracy of the fault characteristic quantities of current and voltage signals at the time of the fault has been assessed. Still, no more detailed theoretical analysis has been carried out. Literature [20] relies on a microcomputer-based dynamic signal online monitoring sub-system called the DAS fault diagnosis system. A browser/server web system for wind turbine gearbox monitoring is introduced using Java language and ASP network technology. Use the SKF condition monitor to monitor the wind turbine gearbox to find the point of failure [21]. To carry out the basic theoretical research on the fault diagnosis of wind turbines, it is necessary to establish a complete set of wind turbine fault simulation test benches to solve the problems that are difficult to capture, the typical faults, or the fact that the wind turbines are unstable. There are many research documents on wind power generation simulation platforms, and the simulation methods are mainly DC motors and AC motors. Due to the DC commutation and maintenance inconvenience of DC motors, in recent years, AC asynchronous motors have gradually been used to simulate wind turbines. Literature [23] designed and established a set of experimental schemes for simulating wind turbines with asynchronous motors using vector control and constructed a complete wind power generation system experimental platform, including a hardware platform and control software. Literature [16] uses a general-purpose frequency converter + squirrel-cage asynchronous electric mechanism to build a fan simulation experiment platform, and the system is simple to establish. In summary, it can be seen that the sensorless fault diagnosis technology in the field of wind turbine fault diagnosis has a wide range of application prospects. The research in this area is only at the preliminary stage; the technology is not yet mature, and there is no use for finalized products. [2]. Since the main model of the wind power generation system adopts a double-fed wound asynchronous generator, which is very similar in structure and principle to an asynchronous motor, it can learn from the fruitful research results of the sensorless fault diagnosis method for the fault diagnosis of asynchronous motors and drive systems. Conduct basic theoretical and experimental research on sensorless diagnosis methods for wind power generation systems, explore the feasibility of sensorless detection technology for mechanical fault diagnosis of wind turbine transmission systems, and provide a solid foundation for its application in wind turbine fault diagnosis. Theoretical basis [11]. The research and application of this technology can effectively solve the technical bottleneck encountered in applying vibration detection methods in wind power systems [10].

3 RESEARCH ON THE STATE OF THE GEARBOX STRUCTURE

There are many ways for gears to mesh with each other to transmit energy and speed. The wind turbine gearbox uses a combination of planetary gears and parallel gears to achieve speed increase. This combination method combines the advantages of planetary gears and similar gears. The

planetary gear system is small in size and mass, compact in structure, large in load capacity, high in transmission efficiency, stable in operation, large in transmission ratio, and can realize the synthesis and decomposition of motion. However, the material price is high, the structure is complicated, and the manufacturing and installation are complex. The transmission distance of parallel wheels is relatively long, and the transmission is rather large. In addition, it can change the steering of the driven shaft, so it is widely used in various mechanical equipment. The failure probability of the main components of the gearbox is shown in Figure 1.

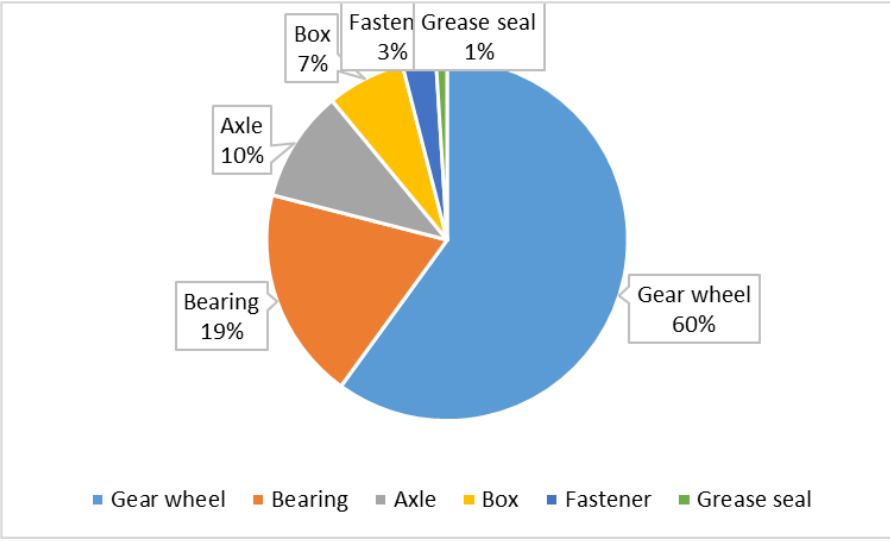

Figure 1: The failure probability of each component of the gearbox.

At present, the gearboxes of wind turbines mainly adopt two transmission structures: one-stage planetary and two-stage parallel structures and two-stage planetary and one-stage parallel structures. The transmission path of the one-stage planetary and two-stage similar gearbox is as follows: the main shaft and the planet carrier are rigidly connected, and the rotational speed is transmitted to the planet carrier. The planetary wheels are fixed on the three branches of the planetary carrier, and the planetary carrier's rotation drives the planetary wheels to revolve around the sun wheel while rotating on the axis. The rotation and revolution of the planetary gear to the sun gear to turn, thereby transferring speed and energy to the sun gear. At this time, the power of the main shaft reaches the sun gear, and the function of the planetary gear system is realized. The large gear at the end of the sun gear shaft in the planetary gear meshes with the secondary parallel shaft pinion to achieve the purpose of a secondary speed increase, and the mesh of the secondary pinion and the tertiary large gear achieves the third speed increase. In this way, it is transmitted by planetary gears and two-stage parallel shaft gears, and the main shaft speed is output by the high-speed shaft after the speed is increased, as shown in Figure 2. The transmission path of the two-stage planetary gear and the first-stage parallel shaft gear is summarized as follows: The main shaft drives the planet carrier to rotate, and the planet carrier drives the three first-stage planetary gears to rotate and revolve. Because the ring gear is fixed, the planetary gear transmits energy to the first-stage sun gear, which turns the second-stage planet carrier. After that, it passes through the secondary planet carrier, secondary planetary gear, and secondary sun gear. The third-stage parallel shaft gear transmits a high-speed shaft output, as shown in Figure 3.

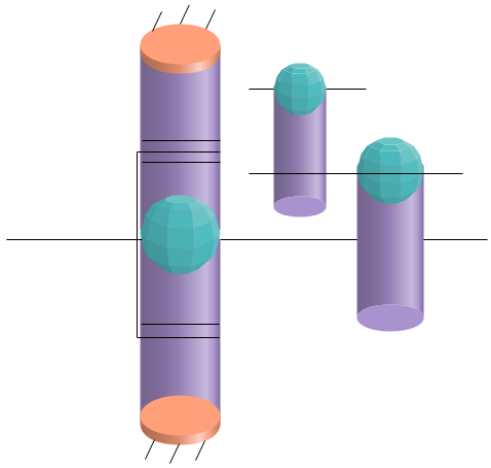

Figure 2: The structure diagram of one-stage planetary and two-stage parallel.

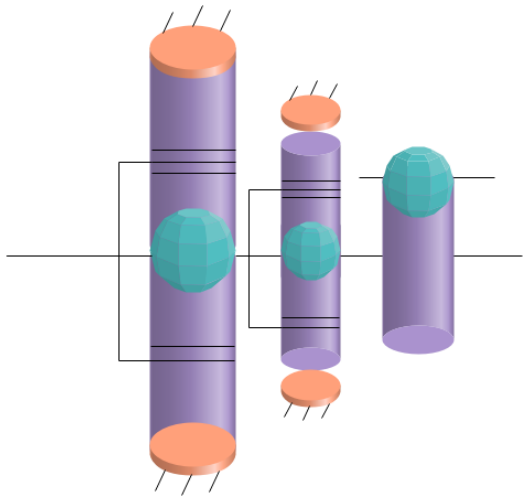

Figure 3: The structure diagram of the two-stage planetary and first-stage parallel.

The fluctuating load on the tooth surface causes the amplitude modulation of the time-domain signal. After the gear is eccentric, when the two wheels mesh, the gear is tight and loose due to the uneven force on the bizarre. The amplitude of the resulting vibration signal changes periodically according to this law, and amplitude modulation occurs. Errors caused by gear processing will also cause the above-mentioned "loading" and "unloading" effects during gear meshing, resulting in amplitude modulation. Generally, amplitude modulation and frequency modulation exist at the same time. Therefore, the vibration signal received by the sensor at the fault point is an amplitude modulation and frequency modulation signal; the amplitude and frequency are modulated, and the fault feature frequency is modulated to the gear meshing frequency and its multiplier. The expression of the gear fault vibration signal is as follows [17]:

$$x(t) = \sum_{k=0}^{\infty} a_k\,(t)\,cos[2\pi k f_m t + b_k(t) + \theta_k] \quad (1)$$

$$a_k(t) = c\sum_{n=0}^{\infty} A_{kn}\cos\left[2\pi n f_g t + \phi_{kn}\right] \quad (2)$$

$$b_k(t) = c\sum_{l=0}^{\infty} B_{kl}\sin\left[2\pi f_g t + \varphi_{kl}\right] \quad (3)$$

Among them, $a_k(t)$、$b_k(t)$ is the amplitude modulation and frequency modulation function, respectively; A_{kn} is the amplitude modulation intensity; B_{kl} is the frequency modulation intensity, c is the dimensionless constant, f_m is the gear engagement frequency, f_g is the fault feature frequency, and $\theta_k, \phi_{kn}, \varphi_{kl}$ is the initial phase.

The planetary gear system generally comprises a ring gear, a planetary gear, a planet carrier, and a sun gear. There are generally three planetary gears. In addition to revolving around the sun gear, they also auto-propagate around the axis, so the planetary gears mesh with the sun gear and the ring gear simultaneously. Usually, the ring gear is fixed, and the planet carrier drives the planetary gear to revolve around the sun gear and drives the sun gear to rotate, realizing the energy transfer from the planet carrier to the sun gear. When measuring the vibration signal of the planetary gear train, the acceleration sensor is installed on the box connected to the ring gear. The ring gear and the box are rigidly connected. It can be approximated that the sensor is installed on the ring gear. There are two gear meshing processes when the planetary gear system works: planetary gear and sun gear. The relative position between the meshing point and the sensor changes with the planet carrier, causing the vibration signal received by the sensor to be an amplitude modulation and frequency modulation signal. When the sun gear fails, the relative position between the fault point and the sensor changes, which modulates the shock vibration caused by the fault. When the planetary gear fails, the auto propagation and revolution cause the relative position of the fault point and the sensor to change, resulting in modulation. When the gear ring fails, the relative position does not change, so only the fault impact force modulates the gear meshing vibration.

An amplitude modulation and a frequency modulation signal can describe the vibration signal of the fault point. The carrier is the meshing frequency and its multiplier, and the modulation frequency is the fault feature frequency of the faulty gear. The expression is as follows:

The sun gear failure is[8]:

$$x(t) = \left[1 - \cos\left(2\pi f_s^{(r)} t\right)\right]\left[1 + A\cos(2\pi f_s t + \phi)\right] \bullet \cos[2n\pi f_m t + B\sin(2\pi f_s t + \varphi) + \theta] \quad (4)$$

The planetary gear failure is:

$$x(t) = [1 - \cos(2\pi f_c t)]\left[1 + A\cos\left(2\pi f_p t + \phi\right)\right] \bullet \cos\left[2n\pi f_m t + B\sin\left(2\pi f_p t + \varphi\right) + \theta\right] \quad (5)$$

The ring gear fault is:

$$x(t) = [1 + A\cos(2\pi f_r t + \phi)] \bullet \cos[2\pi f_m t + B\sin(2\pi f_r t + \varphi) + \theta] \quad (6)$$

Among them, $f_s^{(r)}$ and fc are the absolute rotation frequency of the sun wheel and the planet carrier rotation frequency, respectively. $f_s, f_p,$ and fr are the fault feature frequencies of the sun, planetary, and ring gear, respectively, and f_m is the gear meshing frequency. A, B, and are the intensity of AM and FM, and ϕ, θ is the initial phase.

In the planetary gear system, the meshing frequencies of the sun, planetary, and the planetary and ring gear are the same. The meshing frequency is:

$$f_m = f_c \times z_r = (f_s - f_c)z_s = f_p \times z_p \quad (7)$$

In the formula, f_m is the meshing frequency, f_c is the rotation frequency of the planet carrier, f_s is the rotation frequency of the sun gear, f_p is the rotation frequency of the planet gear, z_s is the number of sun gear teeth, z_p is the number of planet gear teeth, and z_r is the number of ring gear teeth.

1. In the event of a partial failure of the sun gear, within one rotation cycle of the planet carrier, the failure point completes the meshing with all the planet gears. The feature frequency of the local fault is:

$$f_s = \frac{f_m}{z_s} N \tag{8}$$

Z is the number of sun gear teeth, and N is the number of planet gears.

When the sun gear has a distributed failure, within one rotation cycle of the planet carrier, all the faulty parts complete one vibration, and the amplitude and frequency of the vibration change once. The feature frequency of the distributed failure of the sun gear is equal to the rotation frequency of the sun gear.

$$f_s = \frac{f_m}{z_s} \tag{9}$$

Z_s is the number of sun gear teeth, and N is the number of planet gears.

2. When a partial planetary gear failure occurs, within one rotation cycle of the planetary carrier, the failure point meshes with the sun gear and the ring gear, resulting in two impact forces. If two impacts are regarded as one impact, the feature frequency of the local fault is two times the frequency. Its fault feature frequency is

$$f_p = 2\frac{f_m}{z_p} \tag{10}$$

Z_p is the number of planetary gears.

When the planetary gear has a distributed failure, in one rotation cycle of the planet carrier, all the faulty parts complete a vibration, and the amplitude and frequency of the vibration change once. The characteristic frequency of planetary gear distributed failure is:

$$f_p = \frac{f_m}{z_p} \tag{11}$$

Z_p is the number of planetary gears.

3. When a partial failure of the ring gear occurs within one rotation cycle of the planet carrier, the failure point meshes with all the planet gears and generates an impact force. Its fault characteristic frequency is[12]:

$$f_r = \frac{f_m}{z_r} N \tag{12}$$

Z_r is the number of ring gear teeth, and N is the number of planetary gears.

When the gear ring has a distributed failure, within one rotation cycle of the planet carrier, all the faulty parts complete a vibration, and the amplitude and frequency of the vibration change once. The characteristic frequency of distributed faults is:

$$f_r = \frac{f_m}{z_r} \tag{13}$$

$Z_r$is the number of ring gear teeth.

Rolling bearings are an indispensable part of the gearbox, and their primary function is to support high-speed rotating gears. Therefore, the force is complicated, the working environment is harsh, and it is straightforward to damage. The structure of the rolling bearing can be seen from diagrams 2-5. The innermost structure is the inner ring, which is connected to the gear shaft of the gearbox and rotates with the rotation of the gear. The rolling elements are located between the inner ring and the outer ring of the bearing, and it use rolling instead of sliding to reduce the frictional resistance between the inner and outer rings and improve the energy transmission efficiency. The cage is between the rolling elements, and the fixed rolling element positions are kept relatively evenly spaced. The outer ring is located on the outermost side of the bearing and is connected to the bearing seat to encapsulate and protect the bearing.

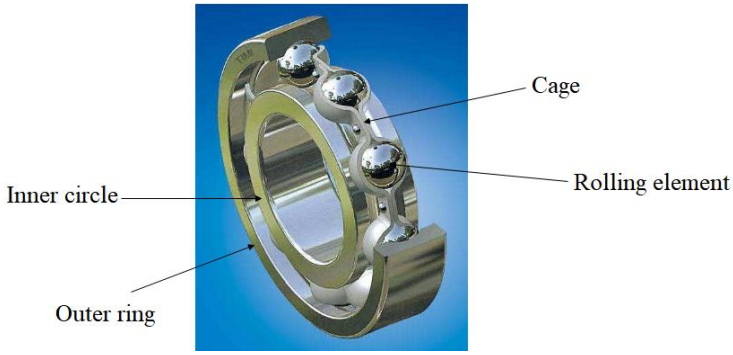

Figure 4: Schematic diagram of rolling bearing structure.

When the rolling bearing fails, the fault point produces periodic impacts. The frequency of the impact force is different for different faulty components so that the positioning of the rolling bearing fault diagnosis can be realized. In actual engineering applications, we don't care about the specific types of failures, such as wear, peeling, or bonding of components. We only need to determine the faulty component in the inner ring, outer ring, cage, or rolling element, so for the judgment of bearing failure, we must first determine which component is faulty. The fault characteristic frequency of each rolling bearing element can be extracted as the basis for determining the bearing fault. The calculation method of the fault's typical frequency is shown below.

The physical parameters of a rolling bearing are shown in Table 1, and the expression of f is as follows:

$$f = \frac{n}{60} \tag{14}$$

In the formula, n is the rotation speed of the shaft. The harmonics of the rotation frequency are Nf, N=1,2,3,...

Table 1 Structural parameters of rolling bearings	*D*	*d*	*Z*	*f*
Contact angle	*Raceway pitch diameter*	*Rolling element diameter*	*Number of rolling elements*	*Rotation frequency*

1. Inner ring fault characteristic frequency:

$$f_i = 0.5Zf\left(1+\frac{d}{D}cos\,\beta\right) \tag{15}$$

2. Outer ring fault characteristic frequency:

$$f_o = 0.5Zf\left(1-\frac{d}{D}cos\,\beta\right) \tag{16}$$

3. Feature frequency of rolling element defects:

$$f_b = \frac{D}{d}f\left[1-\left(\frac{D}{d}\right)^2\cos^2\,\beta\right] \tag{17}$$

4. Unbalance frequency of cage:

$$f_c = 0.5f\left(1-\frac{d}{D}cos\,\beta\right) \tag{18}$$

Monitoring the operating status of the wind turbine gearbox is realized by the characteristic quantities that can characterize the active status of the wind turbine gearbox. Acceleration sensors are now used to monitor the condition of the fan drive system. It measures the vibration signal of each measuring point, analyzes the collected signal in the time domain and frequency domain, extracts the fault characteristics from the signal, and monitors and diagnoses the status of the fan. The time domain parameters of the vibration signal can be used to make an initial judgment on the early failure of the wind turbine operating state. The initial decision is mainly to have a rough judgment on the fault. After the harsh judgment, the fault diagnosis system can determine the fan failure's location and the failure's time.

The practical value, the root mean square, is critical for monitoring the fan gearbox's working status. The practical value is the positive square root of the signal mean honest value, which describes the signal energy's magnitude and reflects the gearbox vibration's severity.

The acquired signal is $x = (x_1, x_2, \cdots, x_N), N = 1,2,3\cdots$, which is substituted into the mean square error formula[18]:

$$X_{rms} = \sqrt{\frac{1}{N}\sum_{i=1}^{N} x_i{}^2} \tag{19}$$

In the formula, X_{rms} is the mean square error value, N is the number of sampling points, $and\ x_n$ is the sampled signal.

The acceleration sensor is used to sample the vibration signal of the fan gearbox, the data and other time segments are used to calculate the practical value of the vibration data in each period, and the observed values in each period are arranged in time to form an effective value sequence diagram. The horizontal axis is time, and the vertical axis is RMS value. When the fan gearbox is in regular operation, the vibration is stable, the practical value amplitude is small, and the change is insignificant. When the gearbox fails, the vibration is severe, and the practical value changes drastically, exceeding the average value several or even dozens of times. The change of the observed value amplitude reflects the development process of the gearbox from average to failure, and the practical value can vividly represent the working status of the fan gearbox.

Fig. 5 shows the time sequence diagram of the practical value of a specific gearbox's three measuring points of 2V, 3A, and 4H. The amplitude of the practical value in the 3A-16K acceleration

effective value graph in the first 1000 hours is below 10mm/s2 (straight line). After 1000 hours, the amplitude exceeds 10mm/s2, and the gearbox is abnormal.

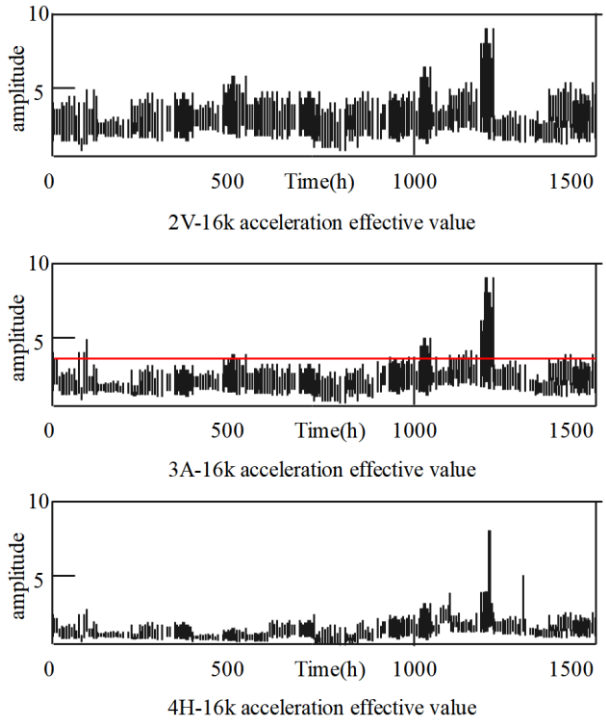

Figure 5: Time sequence diagram of practical value.

Kurtosis is another critical parameter to monitor the working status of wind turbine gearboxes. The formula is as follows:

$$c_q = \frac{1}{N}\sum_{i=1}^{N}\left(\frac{x_i-\mu}{\sigma}\right)^4 \tag{20}$$

In statistics, kurtosis is the fourth-order center distance of a sample, which is used to characterize the degree of convexity of the density cap of the sample. When $c_q = 3$, the sample curve is defined as having normal kurtosis; when $c_q > 3$, the distribution curve is defined as positive kurtosis; when $c_q < 3$, the distribution curve is defined as negative kurtosis.

The kurtosis reflects the impact characteristics in the vibration signal. During the rotating equipment's operation, the vibration signal's amplitude change is close to the normal distribution, and the kurtosis index is $c_q \approx 3$. After the fault occurs, the large amplitude of the vibration signal increases rapidly, and the kurtosis index at this time is $c_q > 3$. The more significant the absolute value of the kurtosis index, the farther away the vibration signal amplitude distribution curve is from the normal state and the more serious the fault. The above is the theoretical basis for gearbox fault diagnosis using the change of kurtosis.

1. Mean

The mean value describes the stable component in the signal and reflects the position of the equilibrium point of mechanical vibration[22].

$$\bar{X} = \frac{1}{N}\sum_{i=1}^{N} x_i \tag{21}$$

2. Peak

The peak value is the single peak maximum value of the vibration waveform. The average value of the n numbers with the most considerable absolute value in the signal.

$$X_p = \frac{1}{n}\sum_{i=1}^{n} X_i \tag{22}$$

3. Crest factor

The crest factor is used to detect whether there is an impact on the signal.

$$P = \frac{\frac{1}{n}\sum_{i=1}^{n} X_i}{\sqrt{\frac{1}{N}\sum_{i=1}^{N} x_i^{\,2}}} = \frac{X_p}{X_{rms}} \tag{23}$$

4. Pulse factor

The impulse factor is used to detect whether there is an impact on the signal, and it is more stable than the crest factor.

$$C_f = \frac{\frac{1}{n}\sum_{i=1}^{n} X_i}{\frac{1}{N}\sum_{i=1}^{N}|x_i|} = \frac{X_p}{|\bar{X}|} \tag{24}$$

5. Margin factor

The margin factor is used to detect the wear and tear of the equipment.

$$C_e = \frac{\frac{1}{n}\sum_{i=1}^{n} X_i}{\left|\frac{1}{N}\sum_{i=1}^{N}\sqrt{|x_i|}\right|^2} = \frac{X_p}{X_r} \tag{25}$$

6. Skewness

Skewness reflects the asymmetry of the vibration signal. Friction or collision in a specific direction causes the asymmetry of the waveform.

$$C_w = \frac{1}{N}\sum_{i=1}^{N}\left(\frac{x_i-\mu}{\sigma}\right)^3 \tag{26}$$

7. Crest factor:

$$F = \frac{\sqrt{\frac{1}{N}\sum_{i=1}^{N} x_i^{\,2}}}{\frac{1}{N}\sum_{i=1}^{N}|x_i|} = \frac{X_{rms}}{|\bar{X}|} \tag{27}$$

The practical value (RMS) of the acceleration signal is one of the critical parameters for monitoring the operating status of the wind turbine gearbox. Its amplitude changes with the change of the gearbox's active state. The gearbox is affected by sudden load and wind speed and sometimes produces high-energy, short-term impact noise. The calculated practical value has serious errors, and the functional value sequence diagram made from this has considerable errors, which reduces the accuracy of the influential value sequence diagram, directly affects the judgment of the gearbox state, and even causes the result of fault misjudgment. Impact noise is non-periodic accidental noise, and the principle of normal distribution 3σ can be used to remove this impact noise effectively.

First, the original vibration signal amplitude is statistically processed to form a histogram. The histogram distribution trend looks like a normal distribution. The average value occupies an absolute proportion and is in the middle part. The shock noise amplitude is abnormally high, accounting for a small proportion, and is at both ends. Then, the standard distribution curve is used to fit the histogram to find the fitted variance. Furthermore, $\mu \pm 3\sigma$ is used as the boundary to eliminate the abnormal data on both sides and finally, the practical value is recalculated with the remaining data.

The probability density of the random variable x is:

$$f(x) = \frac{1}{\sqrt{2\pi}\sigma} e^{-\frac{(x-\mu)^2}{2\sigma^2}} \tag{28}$$

In the formula, π is the ratio of pi, e is the natural index, μ is the average value of the normal population, σ is the standard deviation of the average population, and x is the value of a sample randomly drawn from the average population. It is said that the random variable x obeys the normal distribution with the parameter (μ, σ), denoted by $x \sim N(\mu, \sigma)$.

Affected by a large number of uncertain factors in nature, random variables obey normal distribution. According to the laws of mathematical statistics, it can be known that when the sample size is large enough, the distribution of random variables is similar to the normal distribution. The sampling frequency of the vibration signal of the gearbox is very high. In a certain period, many data points are collected, so the amplitude of the vibration signal obeys the normal distribution.

The 3σ principle is an essential characteristic of the normal distribution, and its content is as follows:

$$P(\mu - \sigma < x < \mu + \sigma) = 68.26\% \tag{29}$$

$$P(\mu - 2\sigma < x < \mu + 2\sigma) = 95.45\% \tag{30}$$

$$P(\mu - 3\sigma < x < \mu + 3\sigma) = 99.73\% \tag{31}$$

That is, available$(\mu - \sigma, \mu + \sigma)$ contains 68.26% of the original data, $(\mu - 2\sigma, \mu + 2\sigma)$ has 95.45% of the original data, and $(\mu - 3\sigma, \mu + 3\sigma)$ contains 99.73% of the original data, as shown in Figure 6.

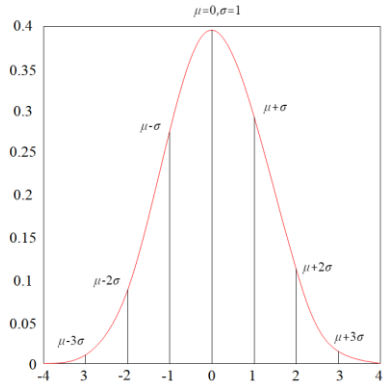

Figure 6: Normal distribution curve.

The acceleration of the wind turbine gearbox is usually distributed within a certain period. We perform statistical processing on the acceleration signal, draw a histogram, and fit it with a standard distribution curve. Since $(\mu - 3\sigma, \mu + 3\sigma)$ contains 99.73% of the original data, the spike noise on both

available can be considered noise. $(\mu - 3\sigma, \mu + 3\sigma)$ is used as the boundary to remove the data at both ends. The practical value is recalculated with the remaining data.

4 RESEARCH ON CONDITION MONITORING AND FAULT DIAGNOSIS OF GEARBOX OF DOUBLY-FED WIND TURBINE BASED ON ARTIFICIAL INTELLIGENCE TECHNOLOGY

The principle of intelligent fault diagnosis for the gearbox of a wind turbine generator is shown in Figure 7(a), and Figure 7(b) shows the development process of the fault diagnostic instrument. According to the basic principles and methods of wind power gearbox fault diagnosis, the functional requirements of the fault diagnosis instrument are put forward. Then, the core software and hardware platform is selected on this basis. With the above two steps as the foundation, since the wind power gearbox fault diagnosis instrument is essentially an embedded system, developing and designing an embedded system must include software and hardware. The hardware part of the whole wind power gearbox fault diagnosis instrument is based on the ARM processor platform. Then, based on the minimum system of the ARM microprocessor, the related peripheral interface circuit is expanded to form the hardware part of the diagnostic instrument. Figure 7 (c) shows the fault diagnosis instrument's hardware structure block diagram.

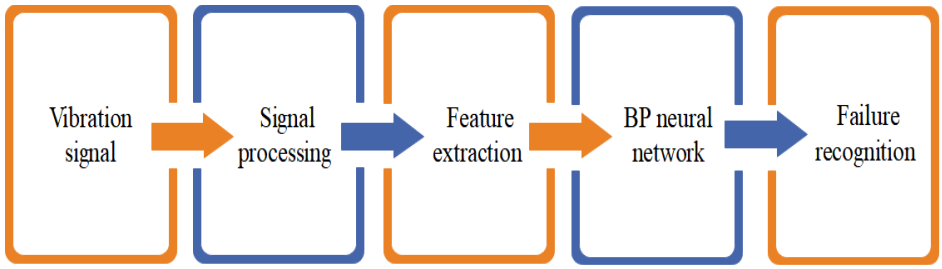

(a) Principles of intelligent fault diagnosis for gearboxes of wind turbines

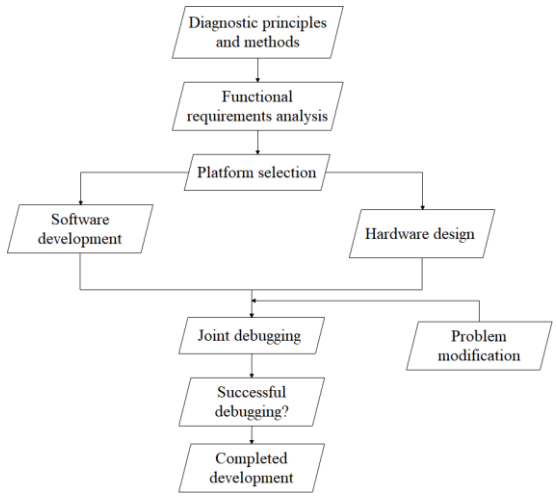

(b) Flow chart of research and development of fault diagnosis system

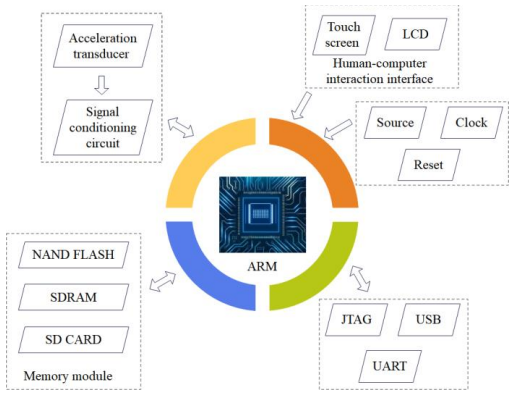

(c) The overall hardware structure block diagram of the system

Figure 7: The Condition Monitoring and Fault Diagnosis System of the Gearbox of the Doubly-Fed Wind Turbine Based on Artificial Intelligence Technology.

Based on the above research, the simulation experiment of the model in this paper is carried out. The simulation is carried out on the four working conditions, and the results shown in Figure 8 below are obtained.

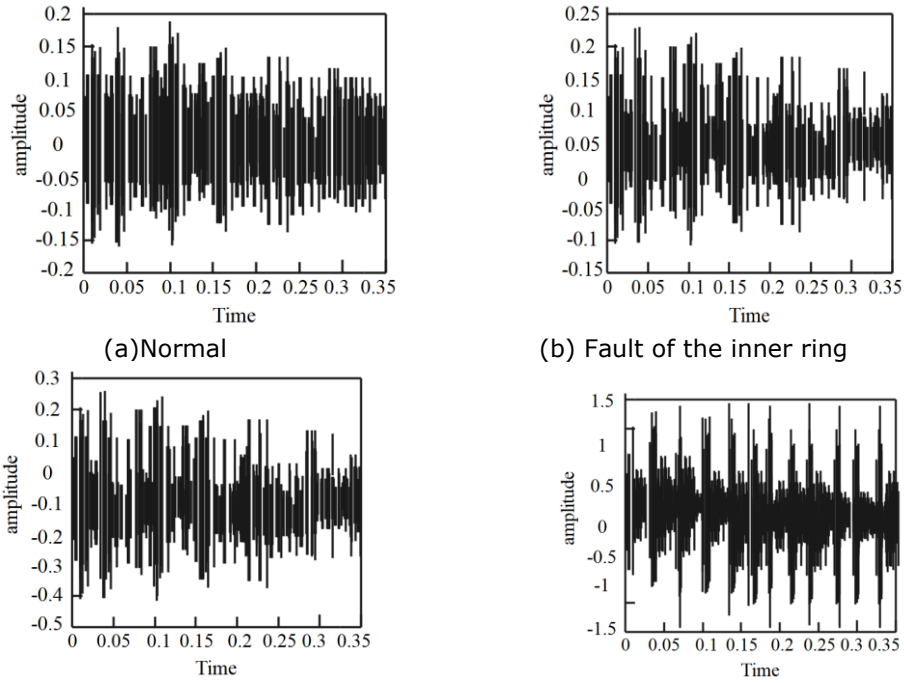

(a)Normal (b) Fault of the inner ring

(c) Fault of rolling body (d) Fault of the outer ring

Figure 8: Time-domain waveforms of four working conditions.

From the energy spectra of the above four working conditions, it can be seen that after the bearing fails, the energy of a particular frequency band will suddenly increase, and the power will be lower under normal conditions. When the inner ring, outer ring, and rolling elements have a fault, the energy value suddenly increases, and the frequency band contains the fault frequency at the corresponding position. It shows that the system proposed in this paper can effectively extract the fault features.

5 CONCLUSION

In the work process of the wind turbine, the manufacturing of parts, the device's accuracy, poor daily maintenance, and operator errors may cause gearbox failures. Researching the fault diagnosis of the wind turbine gearbox can effectively prevent the reduction of the gearbox's working accuracy and reduce or eliminate the occurrence of accidents. Moreover, it maximizes the working potential of bearings and gears, improves production efficiency, and ensures industrial production's safe and efficient operation. Therefore, diagnosing the fault in the wind turbine gearbox is of greater practical significance. In particular, it has significant practical value for reducing the maintenance cost of wind farms on remote islands and improving the operation level. This paper combines artificial intelligence technology to detect the state of the gearbox of the doubly-fed wind turbine and whether there is a fault. The simulation test results show that the intelligent system proposed in this paper can effectively extract the fault characteristics of the doubly-fed wind turbine. This research has delved into the intersection of artificial intelligence (AI) technology, wind turbine mechanics, and human-computer Interaction perspectives to explore how advancements in AI can enhance the reliability of renewable energy systems, particularly in the context of diverse cultural approaches to maintenance and technology adoption.

Ting Wang, https://orcid.org/0009-0003-9169-0050
Zhi-Hui Liu, https://orcid.org/0009-0000-0458-4240
Jing Fan, https://orcid.org/0009-0007-2572-4813

REFERENCES

[1] Artigao, E.; Honrubia-Escribano, A.; Gómez-Lázaro, E.: In-Service Wind Turbine DFIG Diagnosis Using Current Signature Analysis, IEEE Transactions on Industrial Electronics, 67(3), 2019, 2262-2271. https://doi.org/10.1109/TIE.2019.2905821
[2] Chen, F.; Fu, Z.; Yang, Z.: Research on Intelligent Fault Identification Technology of Wind Turbine Supported by Fault Knowledge Base, AMSE Journals-AMSE IIETA Publication-2017-Series: Modelling A, 90(1), 2017, 1-15. https://doi.org/10.18280/mmc_a.900101
[3] Chen, X.; Xu, W.; Liu, Y.; Islam, M. R.: Bearing Corrosion Failure Diagnosis of Doubly Fed Induction Generator in Wind Turbines Based on Stator Current Analysis, IEEE Transactions on Industrial Electronics, 67(5), 2019, 3419-3430. https://doi.org/10.1109/TIE.2019.2917418
[4] Cheng, F.; Qu, L.; Qiao, W.; Hao, L.: Enhanced Particle Filtering For Bearing Remaining Useful Life Prediction of Wind Turbine Drivetrain Gearboxes, IEEE Transactions on Industrial Electronics, 66(6), 2018, 4738-4748. https://doi.org/10.1109/TIE.2018.2866057
[5] Cheng, F.; Qu, L.; Qiao, W.; Wei, C.; Hao, L.: Fault Diagnosis of Wind Turbine Gearboxes Based on DFIG Stator Current Envelope Analysis, IEEE Transactions on Sustainable Energy, 10(3), 2018, 1044-1053. https://doi.org/10.1109/TSTE.2018.2859764
[6] Dameshghi, A.; Refan, M. H.: Wind Turbine Gearbox Condition Monitoring and Fault Diagnosis Based on Multi-Sensor Information Fusion of SCADA and DSER-PSO-WRVM Method, International Journal of Modelling and Simulation, 39(1), 2019, 48-72. https://doi.org/10.1080/02286203.2018.1476008
[7] Dameshghi, A.; Refan, M. H.; Amiri, P.: Wind Turbine Doubly Fed Induction Generator Rotor

Electrical Asymmetry Detection Based on an Adaptive Least Mean Squares Filtering of Wavelet Transform, Wind Engineering, 45(2), 2021, 138-159. https://doi.org/10.1177/0309524X19877525

[8] EMEKSİZ, C.; DOĞAN, Z.; Mehmet, A. K. A. R.; HEKİM, M.: Some Prognostic and Diagnostic Methods for Determining Wind Turbine Failures-A Review, Erzincan Üniversitesi Fen BilimleriEnstitüsüDergisi, 10(2), 2017, 168-183.

[9] Gu, H.; Liu, W. Y.; Gao, Q. W.; Zhang, Y.: A Review on Wind Turbines Gearbox Fault Diagnosis Methods, Journal of Vibroengineering, 23(1), 2021, 26-43. https://doi.org/10.21595/jve.2020.20178

[10] Hashemi, Z.; Rahideh, A.: Rotor Electrical Fault Detection of Wind Turbine Induction Generators Using an Unscented Kalman Filter, Iranian Journal of Science and Technology, Transactions of Electrical Engineering, 44(2), 2020, 979-988. https://doi.org/10.1007/s40998-019-00282-8

[11] Hu, A.; Xiang, L.; Zhu, L.: An Engineering Condition Indicator for Condition Monitoring of Wind Turbine Bearings, Wind Energy, 23(2), 2020, 207-219. https://doi.org/10.1002/we.2423

[12] Li, J.; Li, Q.; Zhu, J.: Health Condition Assessment of Wind Turbine Generators Based on Supervisory Control and Data Acquisition Data, IET Renewable Power Generation, 13(8), 2019, 1343-1350. https://doi.org/10.1049/iet-rpg.2018.5504

[13] Nejad, A. R.; Odgaard, P. F.; Moan, T.: Conceptual Study of a Gearbox Fault Detection Method Applied on a 5-MW Spar-Type Floating Wind Turbine, Wind Energy, 21(11), 2018, 1064-1075. https://doi.org/10.1002/we.2213

[14] Qian, P.; Ma, X.; Cross, P.: Integrated Data-Driven Model-Based Approach to Condition Monitoring of the Wind Turbine Gearbox, IET Renewable Power Generation, 11(9), 2017, 1177-1185. https://doi.org/10.1049/iet-rpg.2016.0216

[15] Qiao, W.; Qu, L.: Prognostic Condition Monitoring for Wind Turbine Drivetrains Via Generator Current Analysis, Chinese Journal of Electrical Engineering, 4(3), 2018, 80-89. https://doi.org/10.23919/CJEE.2018.8471293

[16] Sheng, X.; Wan, S.; Cheng, L.; Li, Y.: Blade Aerodynamic Asymmetry Fault Analysis and Diagnosis of Wind Turbines with Doubly Fed Induction Generator, Journal of Mechanical Science and Technology, 31(10), 2017, 5011-5020. https://doi.org/10.1007/s12206-017-0949-8

[17] Taherian-Fard, E.; Sahebi, R.; Niknam, T.; Izadian, A.; Shasadeghi, M.: Wind Turbine Drivetrain Technologies, IEEE Transactions on Industry Applications, 56(2), 2020, 1729-1741. https://doi.org/10.1109/TIA.2020.2966169

[18] Turnbull, A.; Carroll, J.; McDonald, A.: Combining SCADA and Vibration Data into a Single Anomaly Detection Model to Predict Wind Turbine Component Failure, Wind Energy, 24(3), 2021, 197-211. https://doi.org/10.1002/we.2567

[19] Wang, J.; Cheng, F.; Qiao, W.; Qu, L.: Multiscale Filtering Reconstruction for Wind Turbine Gearbox Fault Diagnosis Under Varying-Speed and Noisy Conditions, IEEE Transactions on Industrial Electronics, 65(5), 2017, 4268-4278. https://doi.org/10.1109/TIE.2017.2767520

[20] Wang, X.; Liu, W. Y.; Zhang, Y.; Gu, H.: A Novel Wind Turbine Fault Diagnosis Method Based on Generator Current Analysis, Journal of Vibroengineering, 22(8), 2020, 1758-1769. https://doi.org/10.21595/jve.2020.21336

[21] Wei, S.; Zhang, X.; Xu, Y.; Fu, Y.; Ren, Z.; Li, F.: Extended Park's Vector Method in Early Inter-Turn Short Circuit Fault Detection for the Stator Windings of Shore Wind Doubly-Fed Induction Generators, IET Generation, Transmission & Distribution, 14(18), 2020, 3905-3912. https://doi.org/10.1049/iet-gtd.2020.0127

[22] Zhang, Y.; Li, M.; Dong, Z. Y.; Meng, K.: Probabilistic Anomaly Detection Approach for Data-Driven Wind Turbine Condition Monitoring, CSEE Journal of Power and Energy Systems, 5(2), 2019, 149-158. https://doi.org/10.17775/CSEEJPES.2019.00010

[23] Zhao, L.; Zhou, Y.; Matsuo, I. B.; Korkua, S. K.; Lee, W. J.: The Design of a Remote Online Holistic Monitoring System for a Wind Turbine, IEEE Transactions on Industry Applications, 56(1), 2019, 14-21. https://doi.org/10.1109/TIA.2019.2951088